Musculoskeletal Case of the Day

Stephen F. Hatem[1], Cheryl A. Petersilge, Jung K. Park

Case 1

A 58-year-old man who presented with a several-month history of left leg swelling.

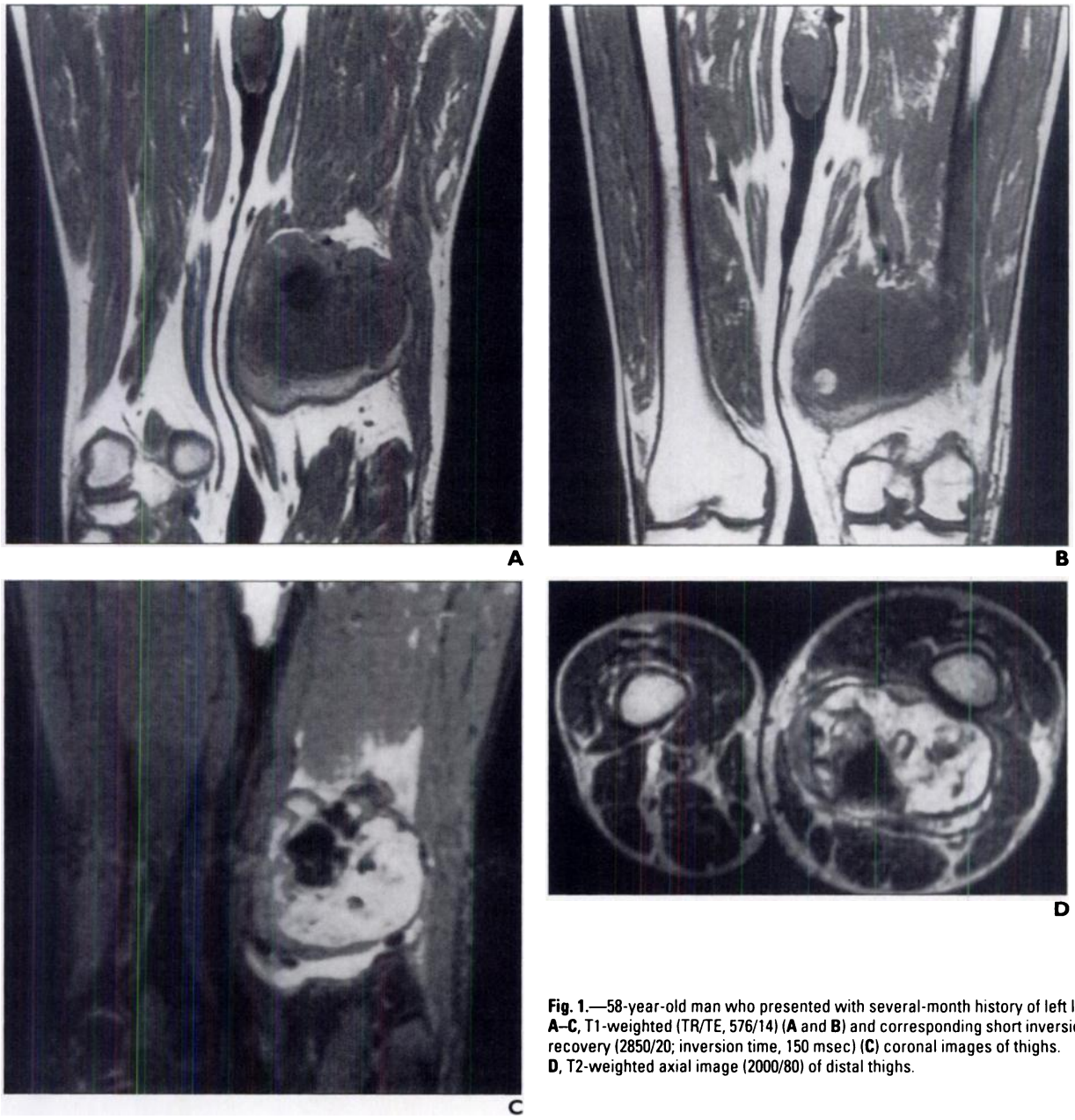

Fig. 1.—58-year-old man who presented with several-month history of left leg swelling.
A–C, T1-weighted (TR/TE, 576/14) (**A** and **B**) and corresponding short inversion time inversion recovery (2850/20; inversion time, 150 msec) (**C**) coronal images of thighs.
D, T2-weighted axial image (2000/80) of distal thighs.

[1] All authors: Department of Radiology, University Hospitals of Cleveland, 11100 Euclid Ave., Cleveland, OH 44106. Address correspondence to S.F. Hatem.

AJR 1997;169:283–292 0361–803X/97/1691–283

Case 2

A 72-year-old man who presented with a painless mass in the posterior right thigh.

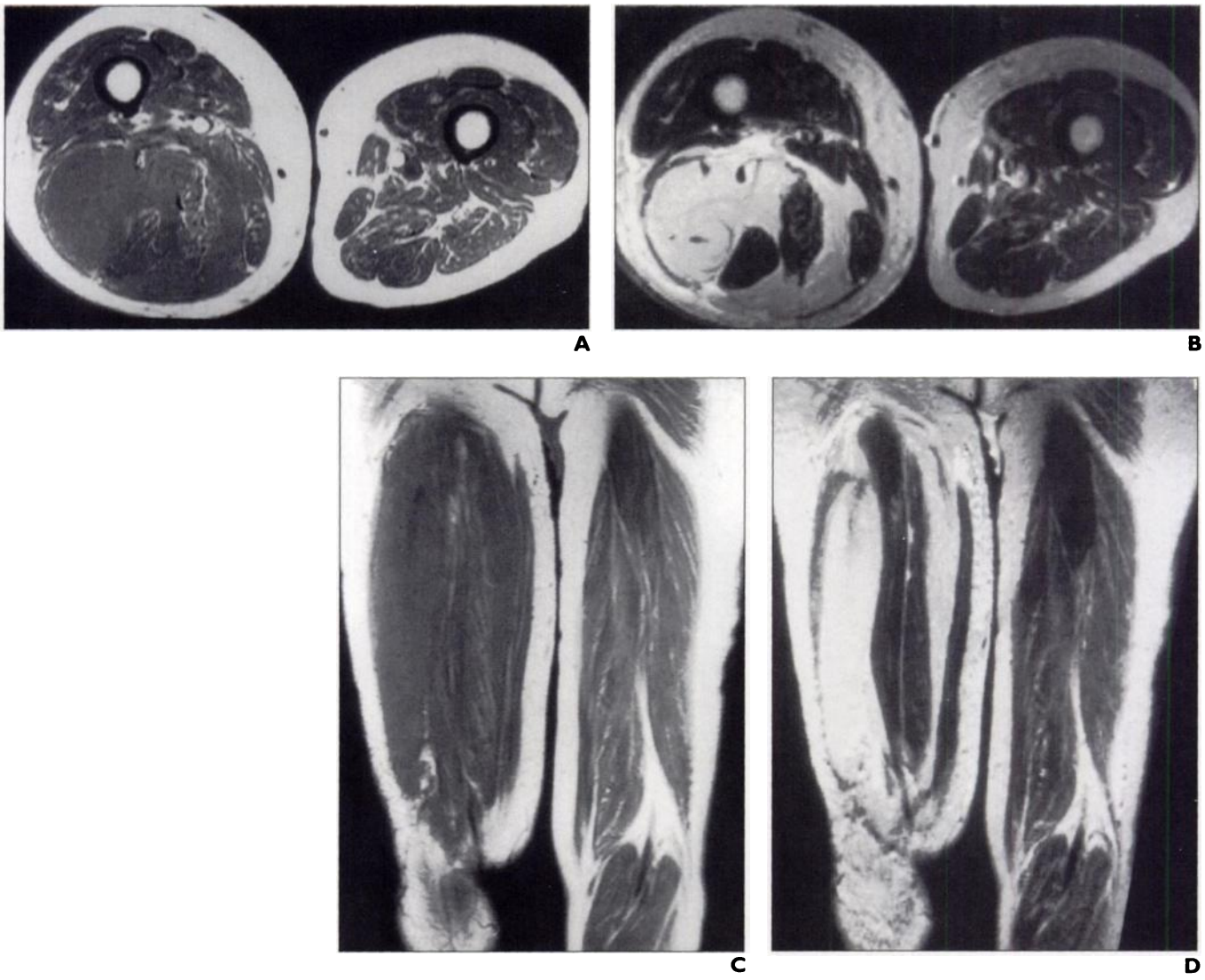

Fig. 2.—72-year-old man who presented with painless mass in posterior right thigh.
A and **B**, T1-weighted (TR/TE, 510/15) (**A**) and T2-weighted (2000/80) (**B**) axial images of mid thighs.
C and **D**, T1-weighted (510/15) (**C**) and T2-weighted (2000/80) (**D**) coronal images through posterior thighs.

Case 3

A 6-year-old girl who presented with progressive swelling and pain over distal left radius for 3 weeks. The pain occasionally wakened her at night.

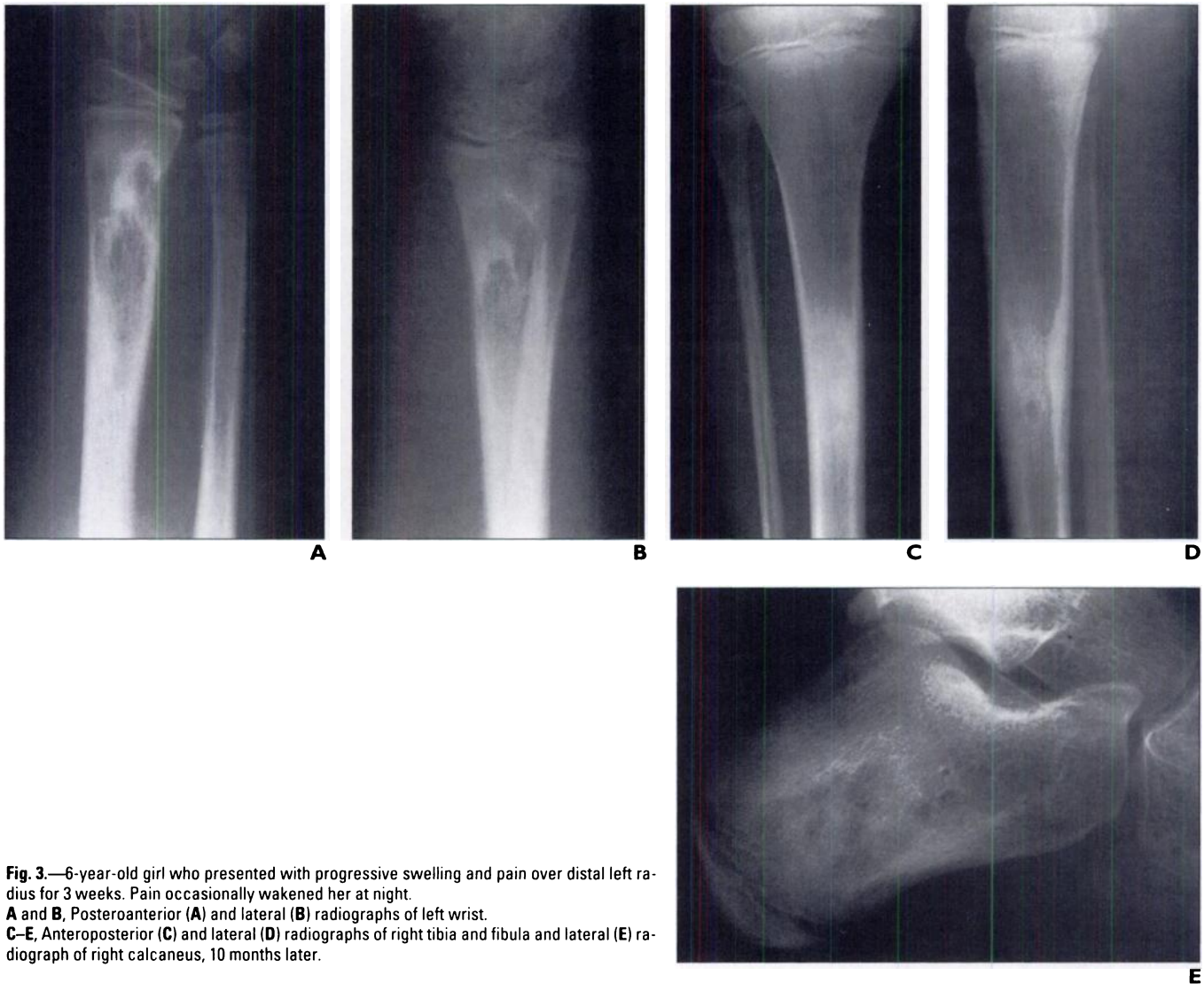

Fig. 3.—6-year-old girl who presented with progressive swelling and pain over distal left radius for 3 weeks. Pain occasionally wakened her at night.
A and **B**, Posteroanterior (**A**) and lateral (**B**) radiographs of left wrist.
C–E, Anteroposterior (**C**) and lateral (**D**) radiographs of right tibia and fibula and lateral (**E**) radiograph of right calcaneus, 10 months later.

Case 4

A 61-year-old man who presented with right knee pain.

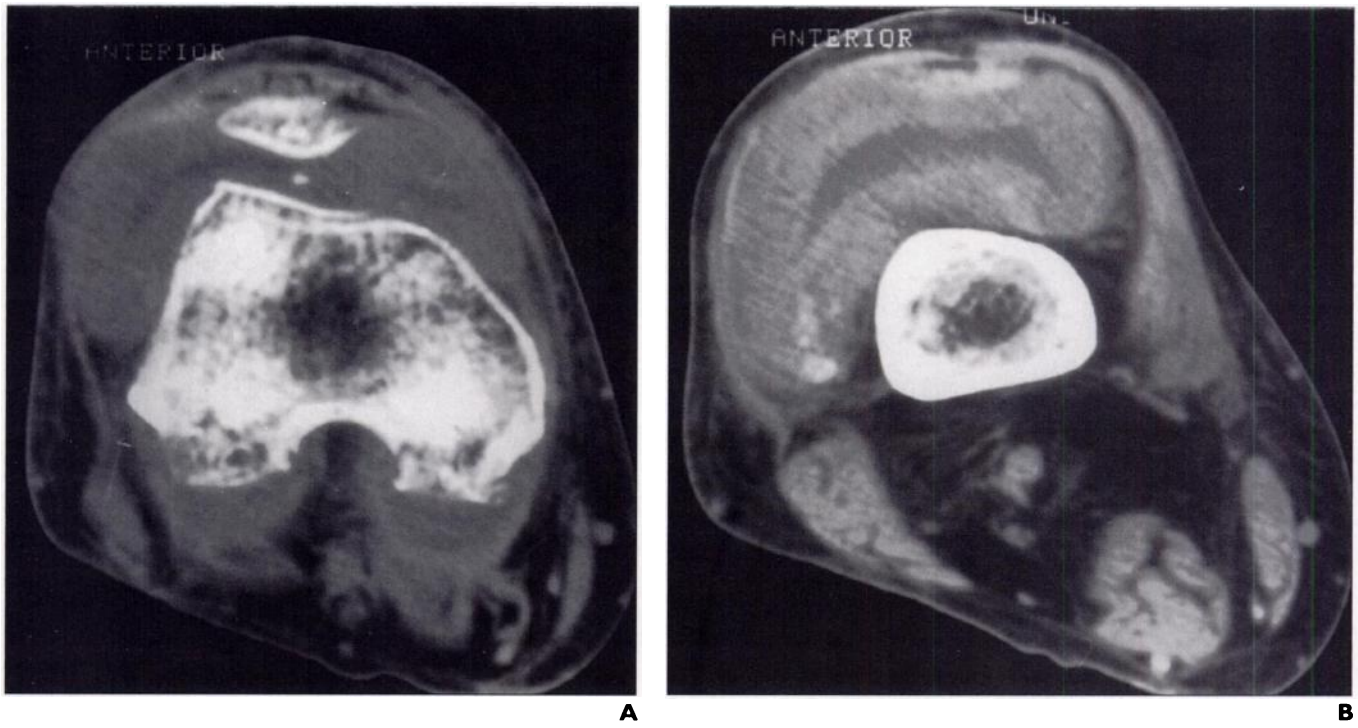

Fig. 4.—61-year-old man who presented with right knee pain.
A and **B**, Axial CT scans of right knee at superior pole of patella (**A**) and supracondylar femur (**B**).

Case 1: Pseudoaneurysm of the Left Superficial Femoral Artery

A pseudoaneurysm, or false aneurysm, results from injury to an arterial wall. As blood leaks from the vessel, a hematoma forms adjacent to the injury, sealing the arterial wall defect. As the hematoma ages, it can liquefy, again allowing free communication with the vessel lumen. Flow from the vascular defect extends into a confined space bounded by clot and adjacent fibrosis. The resultant mass may remain asymptomatic, may enlarge (causing secondary effects due to neurologic or venous compression), or may rupture. If the mass is large enough, peripheral arterial flow can be compromised [1].

The classic clinical presentation of a pseudoaneurysm is a pulsatile mass in a patient with a history of trauma, catheterization, or surgery. This constellation of findings usually allows an accurate clinical diagnosis. However, without this history, or when the mass is nonpulsatile on physical examination (due to a relatively small jet amidst a large hematoma), the diagnosis may not be clinically apparent [2].

Radiographically, a pseudoaneurysm appears as a nonspecific soft-tissue mass. Occasionally, punctate or curvilinear mural calcifications can be seen, particularly on CT [3]. Angiography is the traditional mode for obtaining a diagnosis. A jet of contrast material will be seen extending from the vessel wall into an ill-defined space. However, the overall size of the pseudoaneurysm is not accurately depicted at angiography because of the unopacified thrombus. In recent years, Doppler sonography has become the diagnostic technique of choice, particularly in cases related to femoral artery catheterization. Graded compression techniques have proven useful for treatment by initiating thrombosis at the vessel defect [4].

The appearance of extremity pseudoaneurysms at MR imaging has been reported [5, 6]. A soft-tissue mass is present adjacent to an artery with a persistent flow void on all spin-echo sequences. This signal void extends toward the center of the mass from its origin at the defect in the vessel wall. More peripherally, areas of increased signal intensity related to slow-flowing blood or subacute blood products are seen on T1-weighted images. Concentric zones of homogeneous signal intensity attributed to the different layers of aging thrombus are also seen in Figures 1A and 1B. A low-signal-intensity rim related to fibrous encapsulation or rim calcification may be present [5, 7]. Pulsation and flow artifacts can also be seen, as in the case presented.

The differential diagnosis at MR imaging includes both benign and malignant soft-tissue masses. Hematomas of various ages, including myositis ossificans, can show similar findings with the exception of the flow void. Sarcomas often have a heterogeneous appearance with a pseudocapsule and evidence of blood breakdown products in areas of tumor necrosis and hemorrhage. A flow void should not be seen, and the concentric zonal pattern usually will not be present in sarcomas.

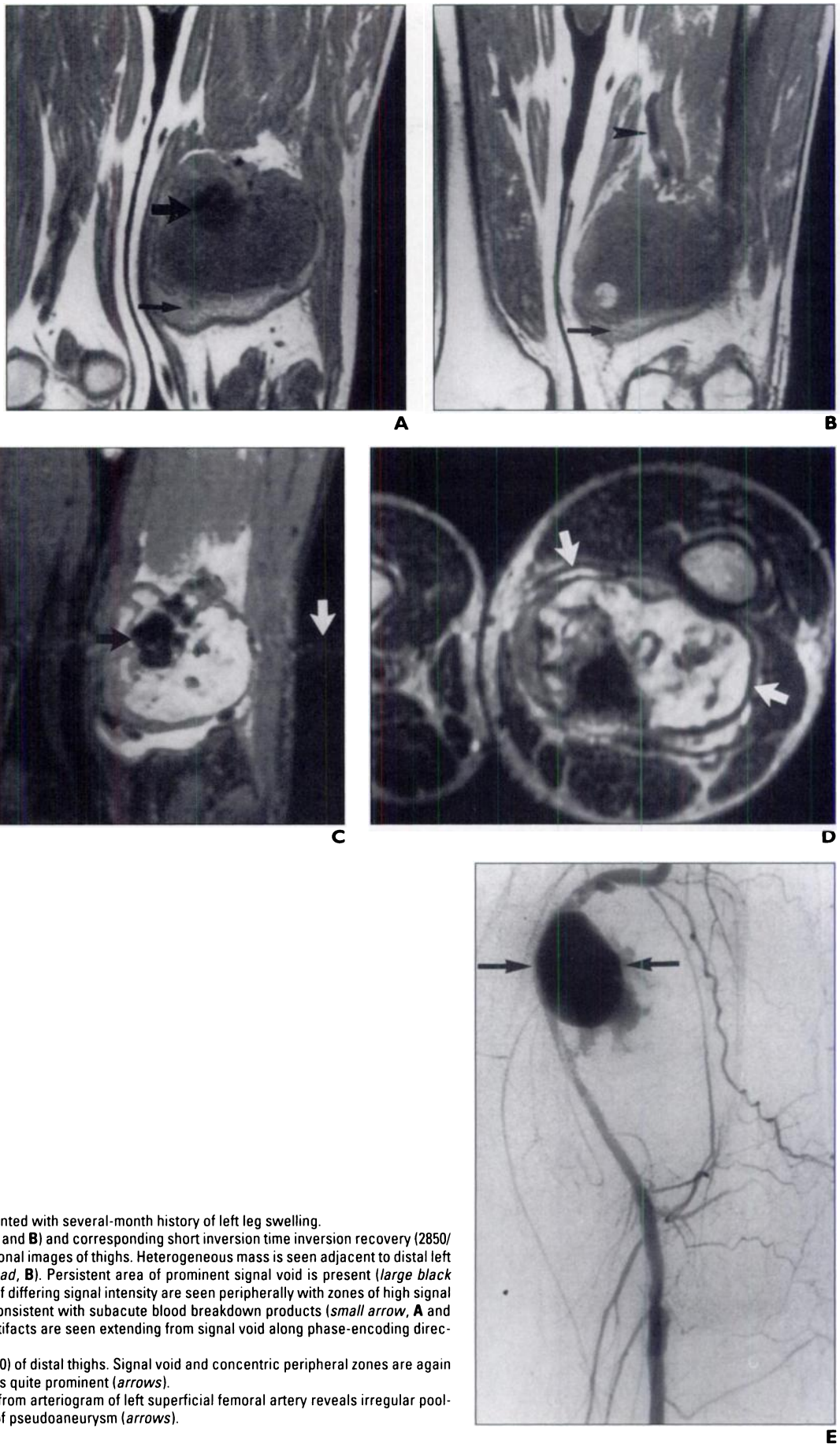

Fig. 1.—58-year-old man who presented with several-month history of left leg swelling.
A–C, T1-weighted (TR/TE, 576/14) (**A** and **B**) and corresponding short inversion time inversion recovery (2850/20; inversion time, 150 msec) (**C**) coronal images of thighs. Heterogeneous mass is seen adjacent to distal left superficial femoral artery (*arrowhead*, **B**). Persistent area of prominent signal void is present (*large black arrow*, **A** and **C**). Concentric zones of differing signal intensity are seen peripherally with zones of high signal intensity on T1-weighted images, consistent with subacute blood breakdown products (*small arrow*, **A** and **B**). Prominent pulsation and flow artifacts are seen extending from signal void along phase-encoding direction (*white arrows*, **C**).
D, T2-weighted axial images (2000/80) of distal thighs. Signal void and concentric peripheral zones are again identified. Low-signal-intensity rim is quite prominent (*arrows*).
E, Right anterior oblique projection from arteriogram of left superficial femoral artery reveals irregular pooling of contrast material into cavity of pseudoaneurysm (*arrows*).

The case presented shows typical MR findings of a pseudoaneurysm. A soft-tissue mass is seen adjacent to the left superficial femoral artery near the adductor canal. On both T1- and T2-weighted images, a flow void is seen adjacent to the vessel, with extension into the center of the mass (Figs. 1A–1C). Foci of high signal intensity related to subacute clot are seen on T1-weighted images. Concentric peripheral zones of aging thrombus are noted on all sequences. Pulsation and flow artifacts are prominent. The diagnosis of pseudoaneurysm was confirmed with angiography, and the patient underwent successful surgical repair.

References

1. Schwartz SI, Shires GT, Spencer FL, Storer EH. *Principles of surgery*, 3rd ed. New York: McGraw–Hill, **1979**:972–973
2. Bole PV, Munda R, Purdy TR, et al. Traumatic pseudoaneurysms: a review of 32 cases. *J Trauma* **1976**;16:63–70
3. Heiken JP, Lee JK, Smathers RL, Totty WG, Murphy WA. CT of benign soft tissue masses of the extremities. *AJR* **1984**;142:575–580
4. Fellmeth BD, Roberts AC, Bookstein JJ, et al. Postangiographic femoral artery injuries: nonsurgical repair with US-guided compression. *Radiology* **1991**;178:671–675
5. Ludwig WD, Yuh WT, Montgomery WJ. Case report: MR imaging of post-traumatic pseudoaneurysm of the deep femoral artery. *J Comput Assist Tomogr* **1987**;11:1093–1095
6. Recht MP, Sachs PB, LiPuma J, Clampitt M. Case report: popliteal artery pseudoaneurysm in a patient with hereditary multiple exostoses—MRI and MRA diagnosis. *J Comput Assist Tomogr* **1993**; 17:300–302
7. Kransdorf MJ, Berquist TH. Musculoskeletal neoplasms. In: Berquist TH, ed. *MRI of the musculoskeletal system*, 3rd ed. Philadelphia: Lippincott–Raven, **1996**:799–800

Case 2: Lymphoma of Skeletal Muscle

Three forms of skeletal muscle lymphoma have been described: primary extranodal involvement, secondary involvement in patients with disseminated disease, and secondary involvement by contiguous spread from osseous disease [1]. All forms are rare, but primary involvement is exceptional. Large series have reported muscle involvement in 1.4% of patients, but primary involvement is present in only 0.14% of lymphoma patients [1].

Muscle involvement by lymphoma may present as a discrete mass or, more commonly, as diffuse muscle enlargement [2]. Preservation of intermuscular fat planes has been described [2, 3]. On unenhanced CT, lymphomatous muscle is hypodense to isodense relative to normal muscle. IV administration of contrast agent has been reported to increase the conspicuity of the involved muscle, either by decreased enhancement relative to normal muscle [2] or by diffuse enhancement of the lymphomatous muscle [3]. Adjacent edematous changes in fat and along fascial planes can be seen [3].

The MR appearance of skeletal muscle lymphoma has only rarely been described [1, 4]. Metzler et al. [4] described two patients—one patient with Hodgkin's disease involving the psoas muscles and vertebrae and a second patient with primary non-Hodgkin's lymphoma of the calf. On T2-weighted images, signal intensity is isointense to hypointense to fat and hyperintense to muscle. Hyperintensity relative to muscle was also noted on the images with TR/TE of 500/30. Muscle, fascial, and subcutaneous fat changes were described. Hosono et al. [1] described four patients with non-Hodgkin's lymphoma involving skeletal muscle of the extremities—two cases of thigh involvement and two cases of arm involvement. These authors described enlargement of the involved muscles with preservation of adjacent fat planes, tumor extension along muscle fascicles, and homogeneous enhancement after IV administration of gadolinium. Vessels appeared to be spared. Involved muscles were hyperintense to muscle on T2-weighted images and isointense to slightly hyperintense on T1-weighted images (imaging parameters were not defined, however).

The case we present shows these typical imaging characteristics. The involved muscles are enlarged and diffusely infiltrated with preservation of their normal contours (Figs. 2C and 2D). The signal intensity is isointense to muscle on T1-weighted spin-echo images (510/15) and isointense to fat on T2-weighted spin-echo images (2000/80) (Figs. 2A and 2B). Tubular signal-intensity voids, presumably vessels with high flow, are noted coursing through the involved muscles.

The differential diagnosis of muscle enlargement is lengthy and includes myopathies, muscle infarction, and postdenervation enlargement. The idiopathic inflammatory myopathies are characterized by proximal muscle weakness that is occasionally accompanied by muscle tenderness and rash. MR imaging usually reveals nonspecific changes of edema in affected muscles, in adjacent subcutaneous or intermuscular fat, and occasionally along myofascial planes. Typically, these inflammatory changes are seen in a patchy distribution bilaterally in proximal muscle groups. With chronic inflammation, atrophy and fatty replacement may be seen [5]. Involvement of a single muscle or several muscles in their entirety is unlikely.

Two forms of muscle involvement in sarcoidosis have been described. The myopathic form appears normal at MR imaging. On the other hand, the nodular sarcoid form has a typical MR imaging appearance. Long intramuscular lesions are seen with stellate low signal intensity centrally (dark star appearance) and a high-signal-intensity rim. This appearance creates a characteristic three-striped pattern on T1- and T2-weighted and gadolinium-enhanced images [6].

Skeletal muscle infarction is a rare complication in patients with diabetes [7] and sickle cell anemia [8]. One or several muscles may be involved. The imaging findings are nonspecific with low to slightly increased signal intensity to muscle on T1-weighted images and increased signal intensity on T2-weighted images [7, 8]. Differentiation from infection in these patients may be difficult.

Denervated skeletal muscle typically atrophies and is replaced by fat. Occasionally, however, the muscle enlarges and the patient can present with a mass or swelling. One or several muscles can be diffusely involved. The enlargement can result from true hypertrophy, with increase in size of the muscle fibers, or from pseudohypertrophy, with enlargement by accumulation of fat and connective tissue within the muscle. Petersilge et al. [9] described the MR appearances of both types of hypertrophy. Muscles that have undergone true hypertrophy are enlarged, with signal characteristics identical to those of normal muscle, whereas pseudohypertrophy is seen as an enlarged muscle, with increased signal intensity that corresponds to fat.

References

1. Hosono M, Kobayashi H, Kotoura Y, et al. Involvement of muscle by malignant lymphoma: MR and CT appearances. *J Comput Assist Tomogr* **1995**; 19:455–459
2. Malloy PC, Fishman E, Magid D. Lymphoma of bone, muscle, and skin: CT findings. *AJR* **1992**; 159:805–809
3. Grunshaw ND, Chalmers AG. Skeletal muscle lymphoma. *Clin Radiol* **1992**;45:399–400
4. Metzler JP, Fleckenstein JL, Vuitch F, Frenkel EP. Skeletal muscle lymphoma: MRI evaluation. *Magn Reson Imaging* **1992**;10:491–494
5. Adams EM, Chow CK, Premkumar A, Plotz PH. The idiopathic inflammatory myopathies: spectrum of MR imaging findings. *RadioGraphics* **1995**;15:563–574
6. Otake S. Sarcoidosis involving skeletal muscle: imaging findings and relative value of imaging procedures. *AJR* **1994**;162:369–375
7. Nunez-Hoyo M, Gardner CL, Motta AO, Ashmead

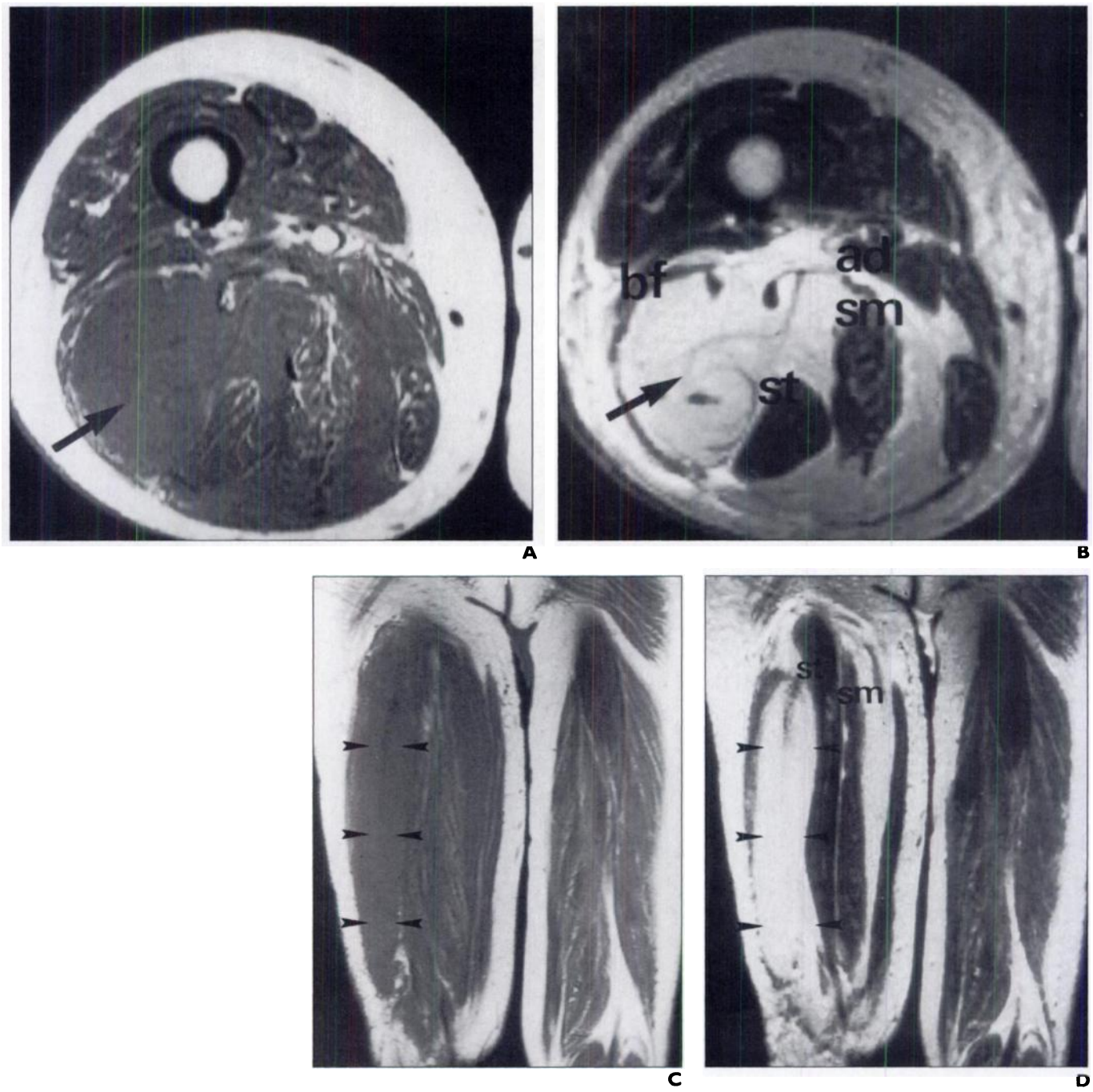

Fig. 2.—72-year-old man who presented with painless mass in posterior right thigh.
A and **B**, T1-weighted (TR/TE, 510/15) (**A**) and T2-weighted (2000/80) (**B**) axial images of mid thighs. Long head of biceps femoris muscle is completely replaced by tissue that is minimally hyperintense to normal muscle and hypointense to fat on T1-weighted images and isointense to fat on T2-weighted images (*arrow*). Tissue engulfs semimembranosus (sm, **B**) and semitendinosus (st, **B**) muscles. Adductor muscles (ad, **B**) and short head of biceps femoris muscle (bf, **B**) are displaced.
C and **D**, T1-weighted (510/15) (**C**) and T2-weighted (2000/80) (**D**) coronal images through posterior thighs. Extension of tumor along preserved fascicles of semimembranosus (sm, **D**) and semitendinosus (st, **D**) muscles is clearly evident as is preservation of muscle bellies. Entire course of long head of biceps femoris is replaced (*arrowheads*).

JW. Skeletal muscle infarction in diabetes: MR findings. *J Comput Assist Tomogr* **1993**;17: 986–988
8. Feldman F, Zwass A, Staron RB, Haramati N. MRI of soft tissue abnormalities: a primary cause of sickle crisis. *Skeletal Radiol* **1993**;22:501–506
9. Petersilge CA, Pathria MN, Gentili A, et al. Denervation hypertrophy of muscle: MR features. *J Comput Tomogr* **1995**;19:596–600

Case 3: Chronic Recurrent Multifocal Osteomyelitis (CRMO)

CRMO is an uncommon subacute and chronic osteomyelitis of unknown cause that usually occurs in children. Similar radiographic and clinical findings have been variably described as subacute symmetric osteomyelitis, chronic multifocal cleidometaphyseal osteomyelitis, plasma cell osteomyelitis, and as part of the synovitis, acne, pustulosis, hyperostosis, and osteitis syndrome. CRMO is characterized by multiple relapsing symptoms and is a self-limited process with minimal residual sequelae. A female predilection exists for this disease,

which is most commonly seen in children and adolescents. However, the age of onset has been reported to range from 20 months old to 55 years old [1]. The characteristic course of exacerbation and remission typically lasts several years [2–4].

The clinical manifestations include pain, focal tenderness, and erythema over the region of osteomyelitis. Mild fever and minimal systemic symptoms are present. Arthralgia and skin changes of palmoplantar pustulosis and psoriasis are associated with this condition. The laboratory findings include an elevated erythrocyte sedimentation rate with a normal or minimally elevated WBC count. Bone biopsy shows changes of osteomyelitis with various degrees of fibrosis and plasma cell, lymphocyte, and histiocyte infiltration. Bone cultures and blood cultures are both negative for pathogens. No association with an immunodeficient state has been established.

The tibia, fibula, femur, and clavicle are the most common sites of involvement (Figs. 3C and 3D). The radius, ulna, foot, and vertebrae are also frequently involved [2, 3, 5]. The lesions are often, but not always, symmetric. The metaphyses of long bones are most commonly involved, similar to the sites of involvement of acute hematogenous osteomyelitis in children and infants. Initially, a well-defined osteolytic lesion with a pyramidal shape or sinuous border is identified near the physis. A thin rim of sclerosis may be seen [3]. Later, extensive peripheral sclerosis develops, which is characteristic of this disease. Frequently, associated soft-tissue swelling is evident. Periosteal reaction is minimal, if present at all. Although most lesions heal completely, some lesions leave residual sclerosis and expansion [2]. The small-diameter bones, such as distal radius and ulna, distal fibula, and clavicle and ribs, present with more extensive periosteal reaction, sclerosis, and soft-tissue swelling compared with the large-diameter bones [6]. Although most lesions typically resolve without clinical sequelae, epiphyseal extension may occasionally cause premature physeal fusion [3, 6]. In addition, sclerosis and expansion around joints can predispose to development of degenerative joint disease [4]. A vertebral lesion causing vertebra plana and progressive kyphosis has been described [2].

Whereas the hallmark of radiographic diagnosis rests with plain film imaging, radionuclide bone scintigraphy can help locate additional lesions. MR imaging findings of CRMO have been described [7, 8]. As expected with most inflammatory processes, the T1-weighted images reveal decreased signal intensity and T2-weighted images reveal increased signal intensity in comparison with the signal intensity of normal marrow [7, 8]. With progression of the disease, conversion to decreased signal intensity on T2-weighted images has been described [7].

The differential diagnosis for the multifocal osteolytic lesions of CRMO in the pediatric population would include bacterial osteomyeli-

Fig. 3.—6-year-old girl who presented with progressive swelling and pain over distal left radius for 3 weeks. Pain occasionally wakened her at night.
A and **B**, Posteroanterior (**A**) and lateral (**B**) radiographs of left wrist show lobulated osteolytic lesion with well-defined borders and surrounding sclerosis in distal radius. Minimal expansion, mild periosteal reaction, and soft-tissue swelling are present.
C–E, Anteroposterior (**C**) and lateral (**D**) radiographs of right tibia and fibula and lateral (**E**) radiograph of right calcaneus, 10 months later. Multiple well-defined osteolytic lesions involving proximal diaphysis of tibia are identified within broad border of sclerosis (*arrows*, **C** and **D**). Similar lesion is identified within posterior calcaneus near physis of posterior apophysis (*arrows*, **E**). No significant periosteal reaction is present.

tis, histiocytosis X (eosinophilic granuloma, Langerhan's histiocytosis), leukemia, and metastatic neuroblastoma. Once a biopsy has been taken and diagnosis has confirmed the absence of malignancy or culture-positive osteomyelitis, CRMO should be the primary consideration. Diagnostic criteria for CRMO have been proposed to include all of the following: the presence of two or more radiographically confirmed bone lesions, a prolonged course of at least 6 months with characteristic exacerbation and remission, radiographic and nuclear scintigraphic evidence of osteomyelitis, a lack of response to antimicrobial therapy for at least 1 month's duration, and the lack of an identifiable cause [6]. A definitive role for steroids or long-term antibiotic use has not been established. Supportive management with antiinflammatory medication is recommended, as the typical course of CRMO is self-limited.

References

1. Rosenberg ZS, Shankman S, Klein M, Lehman W. Chronic recurrent multifocal osteomyelitis. *AJR* **1988**;151:142–144
2. Carr AJ, Cole WG, Roberton DM, Chow CW. Chronic multifocal osteomyelitis. *J Bone Joint Surg Br* **1993**;75-B:582–591
3. Mortensson W, Edeburn G, Fries M, Nilsson R. Chronic recurrent multifocal osteomyelitis in children. *Acta Radiol* **1988**;29:565–570
4. Brown T, Wilkinson RH. Chronic recurrent multifocal osteomyelitis. *Radiology* **1988**;166:493–496
5. Van Howe RS, Starshak RJ, Chusid MJ. Chronic, recurrent multifocal osteomyelitis. *Clin Pediatr (Phila)* **1989**;28:54–59
6. Manson D, Wilmot DM, King S, Laxer RM. Physeal involvement in chronic recurrent multifocal osteomyelitis. *Pediatr Radiol* **1989**;20:76–79
7. Dawson JS, Webb JK, Preston BJ. Case report: chronic recurrent multifocal osteomyelitis with magnetic resonance imaging. *Clin Radiol* **1994**;49:133–136
8. Machiels F, Seynaeve P, Lagey C, Mortelmans LL. Chronic recurrent multifocal osteomyelitis with MR correlation: a case report. *Pediatr Radiol* **1992**;22:535–536

Case 4: Metastatic Carcinomatous Arthritis from Mucinous Adenocarcinoma of the Colon

Rarely, a patient may present with arthritis as a manifestation of a malignancy. Several possible causes exist [1–3]: paraneoplastic syndromes such as hypertrophic osteoarthropathy, Sjögren's syndrome, and the rheumatoid-like carcinomatous polyarthritis; gout; irritative inflammatory arthritis related to a nearby soft-tissue or osseous metastasis; and metastatic carcinomatous arthritis associated with metastatic involvement of the synovium.

Of these causes, metastatic carcinomatous arthritis is the least common and is rare in association with adenocarcinoma as compared with hematologic malignancies [4]. Synovial involvement is usually caused by invasion from an adjacent bone metastasis. Synovial metastasis without adjacent osseous metastasis is rare. To our knowledge, only three cases that specifically identify primary synovial involvement have been reported [1, 2, 5]. Although Benhamou et al. [3] found 19 reported cases of metastatic arthritis associated with adenocarcinoma over a 25-year period, no differentiation was made between direct synovial involvement and contiguous spread.

The most common primary tumor associated with metastatic carcinomatous arthritis is bronchogenic carcinoma, followed by breast and gastrointestinal carcinomas [3, 6]. Monoarticular disease is the rule [6]; the knee is most frequently involved, though involvement of other large and small joints has been reported [3, 6]. Clinically, an effusion is present and the joint appears inflamed [1]. Synovial fluid is usually sanguineous and not consistent with an inflammatory process [6]. Cytologic evaluation may reveal malignant cells [2]. Synovial biopsy is often diagnostic [1, 2].

In addition to clinical findings that mimic arthritis, the radiographic appearance of metastatic carcinomatous arthritis can mimic other entities. The osseous metastases may simulate the periarticular osteopenia, erosions, subchondral cysts, and subchondral sclerosis seen with many arthropathies [1, 5]. In the absence of an osseous lesion, as in the case presented here (Fig. 4), the differential diagnosis of synovial thickening with numerous punctate calcifications and knee joint effusion includes a spectrum of lesions. This spectrum includes synovial osteochondromatosis, calcium pyrophosphate deposition, gout, hydroxyapatite deposition disease, and, as in the case presented here (Fig. 4), metastatic disease.

Synovial osteochondromatosis results from development of nodules of metaplastic carti-

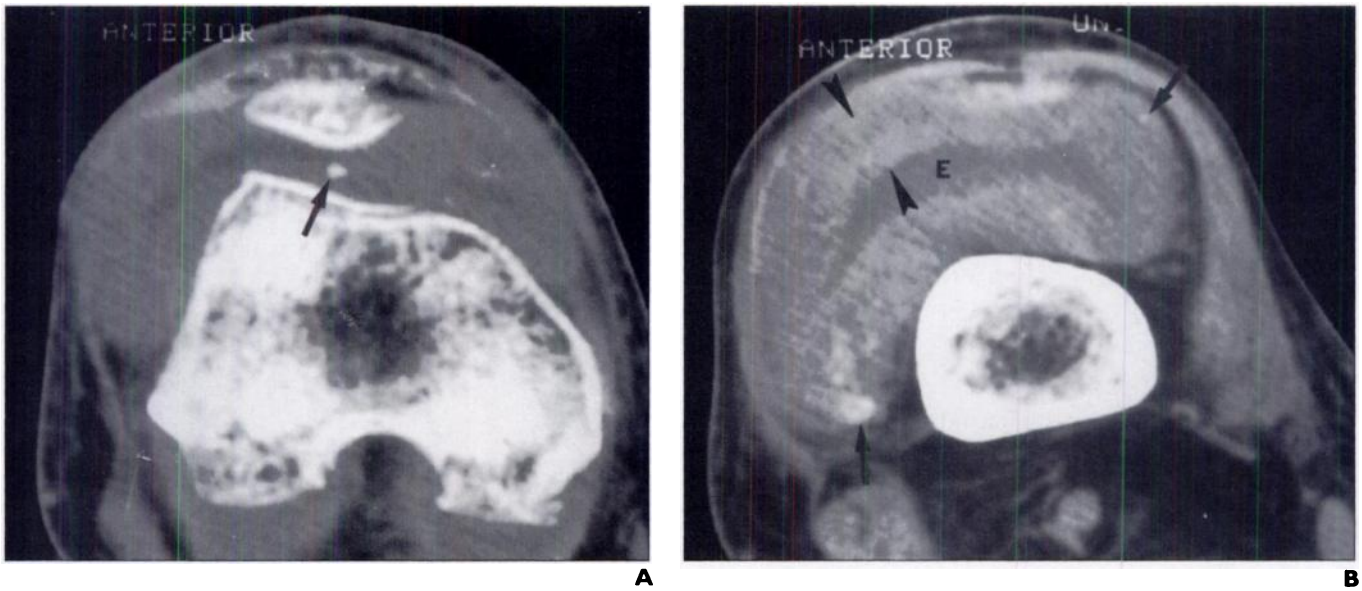

Fig. 4.—61-year-old man who presented with right knee pain.
A and **B**, Axial CT scans of right knee at superior pole of patella (**A**) and supracondylar femur (**B**) show marked synovial thickening (*arrowheads*, **B**) with punctate superficial (*arrow*, **A**) and deep (*arrows*, **B**) calcifications. Joint effusion (**E**, **B**) is evident. Bones show no evidence of metastases.

lage within the synovium [7]. These nodules can ossify and eventually break off to become joint bodies. These bodies typically range in size from several millimeters to several centimeters and have radiolucent centers. The synovium should have a nodular appearance, unlike the smooth appearance shown in Figure 4. A joint effusion is rarely present.

With calcium pyrophosphate deposition, synovial calcifications are unusual in the absence of chondrocalcinosis [7]. However, synovial calcification may occasionally be the most significant finding. These calcifications typically are seen as cloudlike densities located within the superficial layers of the synovium at the joint margins. Capsular calcifications may also be present and usually are linear. Calcifications associated with gout are usually related to tophi or associated calcium pyrophosphate deposition. Although the calcifications of hydroxyapatite deposition disease are usually in the periarticular structures, the calcifications may be found occasionally within the synovium. The calcifications shown in the case presented here (Fig. 4) are present in both the superficial and the deep layers of synovium, an unusual distribution for crystal deposition diseases.

The mineralization that is evident in the case presented in Figure 4 is within the tumor-infiltrated synovium. Soft-tissue mineralization in association with neoplasia has been classified into four types [8]: orthoplastic calcification, in which tumor-produced osteoid matrix mineralizes, as in osteosarcoma; metaplastic calcification, similar to endochondral bone formation, in tumoral cartilage; dystrophic calcification, the most common type, which is thought to represent a local reaction to ischemia, hemorrhage, or necrosis that initiates calcium deposition; and mucoid-type calcification, associated with mucin-secreting carcinomas, which is thought to be related to degradation of glycoproteins and mucopolysaccharides.

Mucoid-type calcification was the presumed cause in the patient presented here, who had biopsy-proven mucinous adenocarcinoma of the colon metastatic to the synovium of his knee.

References

1. Murray GC, Persellin RH. Metastatic carcinoma presenting as monoarticular arthritis: a case report and review of the literature. *Arthritis Rheum* **1980**;23:95–100
2. Goldenberg DL, Kelley W, Gibbons RG. Metastatic adenocarcinoma of synovium presenting as an acute arthritis: diagnosis by closed biopsy. *Arthritis Rheum* **1975**;18:107–110
3. Benhamou CL, Tourliere D, Brigant S, et al. Synovial metastasis of an adenocarcinoma presenting as a shoulder monoarthritis. *J Rheumatol* **1988**;15: 1031–1033
4. Harden EA, Moore JO, Haynes BF. Leukemia-associated arthritis: identification of leukemic cells in synovial fluid using monoclonal and polyclonal antibodies. *Arthritis Rheum* **1984**;27:1306–1308
5. Meals RA, Hungerford DS, Stevens MB. Malignant disease mimicking arthritis of the hip. *JAMA* **1978**;239:1070–1071
6. Fam AG, Kolin A, Lewis AJ. Metastatic carcinomatous arthritis and carcinoma of the lung: a report of two cases diagnosed by synovial fluid cytology. *J Rheumatol* **1980**;7:98–104
7. Resnick D. *Diagnosis of bone and joint disorders*, 3rd ed. Philadelphia: Saunders, **1995**:3982–3993
8. Ferrozzi F, Bova D, De Chiara F, et al. CT of secondary neoplasms: unusual structural features—a pictorial essay. *Clin Imaging* **1995**;19:131–137